Supplemental information for:

Key Role of Nitrogen-containing Oxygenated Organic Molecules (OOMs) in SOA Formation Evidenced by OH/NO_3^- induced Terpinolene Oxidation

Hongjin Wu[1], Juan Dang[1], Xiaomeng Zhang[1], Weichen Yang[1], Shuai Tian[2,3,4], Shibo Zhang[1*], Qingzhu Zhang[1], Wenxing Wang[1]*

1. Environment Research Institute, Shandong University, Qingdao 266237, China

2. Department of Cardiology, The Eighth Affiliated Hospital, Sun Yat-sen University, Shenzhen, Guangdong 518033, China

S1 Volatility Estimation and Classification

The group contribution method, i.e., SIMPOL.1 from the GECKO-A website (https://geckoa.lisa.u-pec.fr), is utilized to estimate the saturated vapor pressure. However, the dataset involved in SIMPOL.1 is limited in the calculation of the contribution of -$OONO_2$ group, except for peroxyacetyl nitrate (PAN). Therefore, we also employed the optimized molecular formula parameterization method to assess the volatility of the OOMs[1, 2], which considers the -OOH functional group of OOMs to enhance predictive accuracy. The governing equation is given below:

$$log_{10}C_0 = (n_c^0 - n_c)b_c - (n_0 - 3n_N)b_0 - 2 \cdot \frac{(n_0 - 3n_N)n_c}{(n_C + n_O - 3n_N)} b_{CO} - n_N b_N$$

Among them, n_c^0=0.475, b_c=0.475, b_0=0.2, b_{CO}=0.9, b_N=2.5.

The OOMs generated by the further oxidation of alkyl radical (Ter-R•) initiated by OH/NO_3 radical from terpinolene was classified according to the volatility classification scheme for organic compounds proposed by Donahue et al.(2012)[3], i.e., ELVOC ($C^* < 3\times10^{-4}$ μg m^{-3}), LVOC ($3\times10^{-4} < C^* < 0.3$ μg m^{-3}), SVOC ($0.3 < C^* <$ 300 μg m^{-3}), intermediate volatility organic compounds (IVOC, $300 < C^* < 3\times10^6$ μg m^{-3}) and volatile organic compounds (VOC, $C^* > 3\times10^6$ μg m^{-3}), of which, ELVOC and LVOC are basically existed in the particulate phase, and SVOC is distributed in both gas phase and particle phase, depending on the atmospheric conditions.

S2 Figures of Initial Reactions of Terpinolene with OH/NO_3 Radical

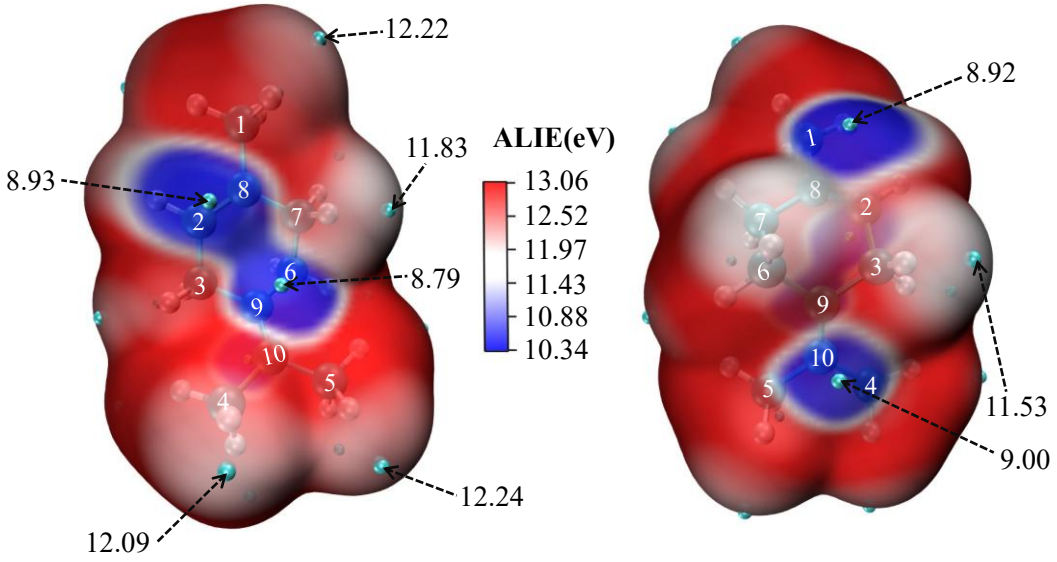

Figure S1. The average local ionization energy of terpinolene

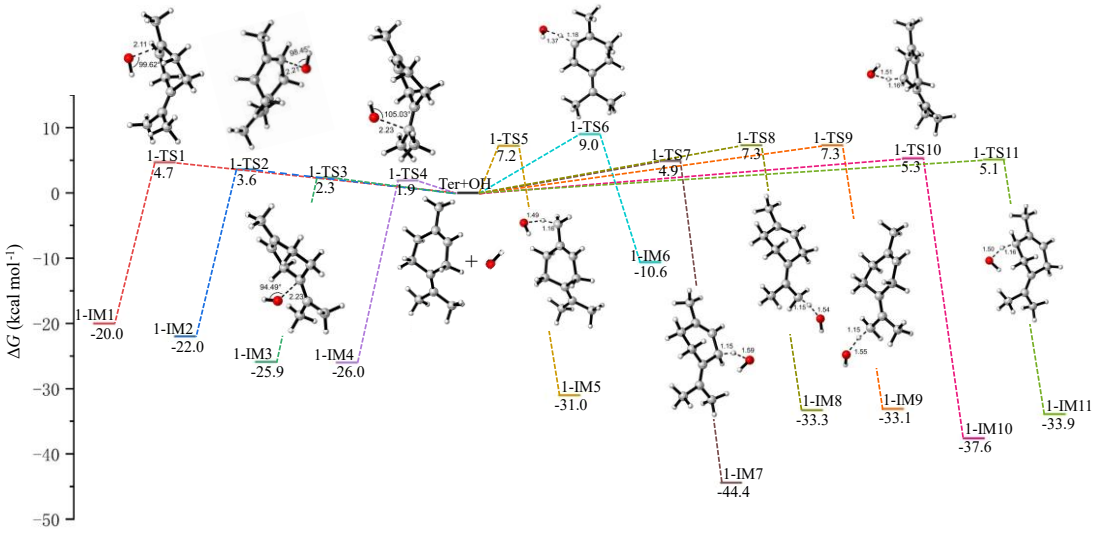

Figure S2. The potential energy profile diagram of initial reactions of terpinolene with OH radical (unit in kcal mol^{-1})

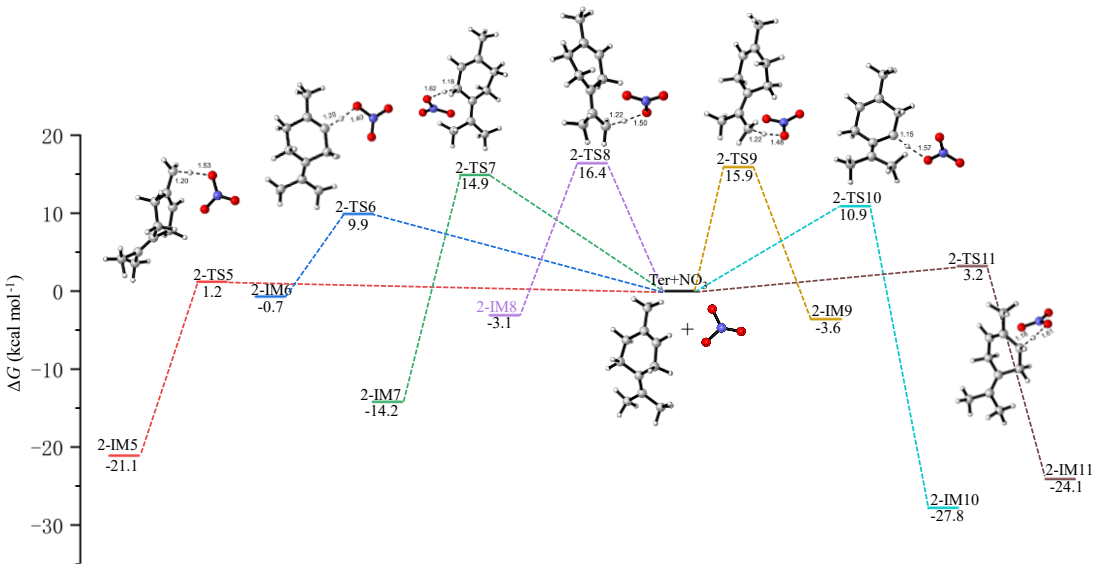

Figure S3. The potential energy profile diagram of H abstraction reactions of terpinolene with NO_3 radical (unit in kcal mol^{-1})

S3 Figures of Atmospheric Oxidation of Alkyl Radical (Ter-R•) Initiated by OH/NO_3 Radical from Terpinolene

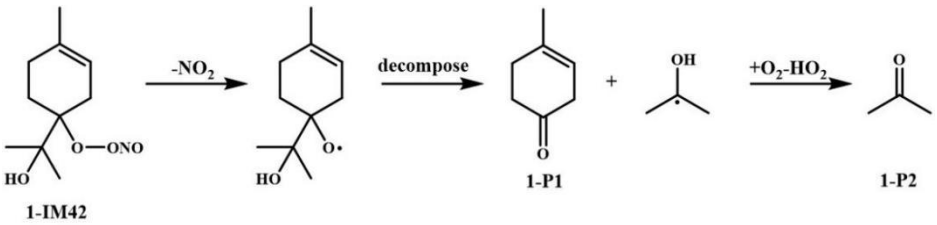

Figure S4. The reaction pathway for NO_2 elimination of IM42

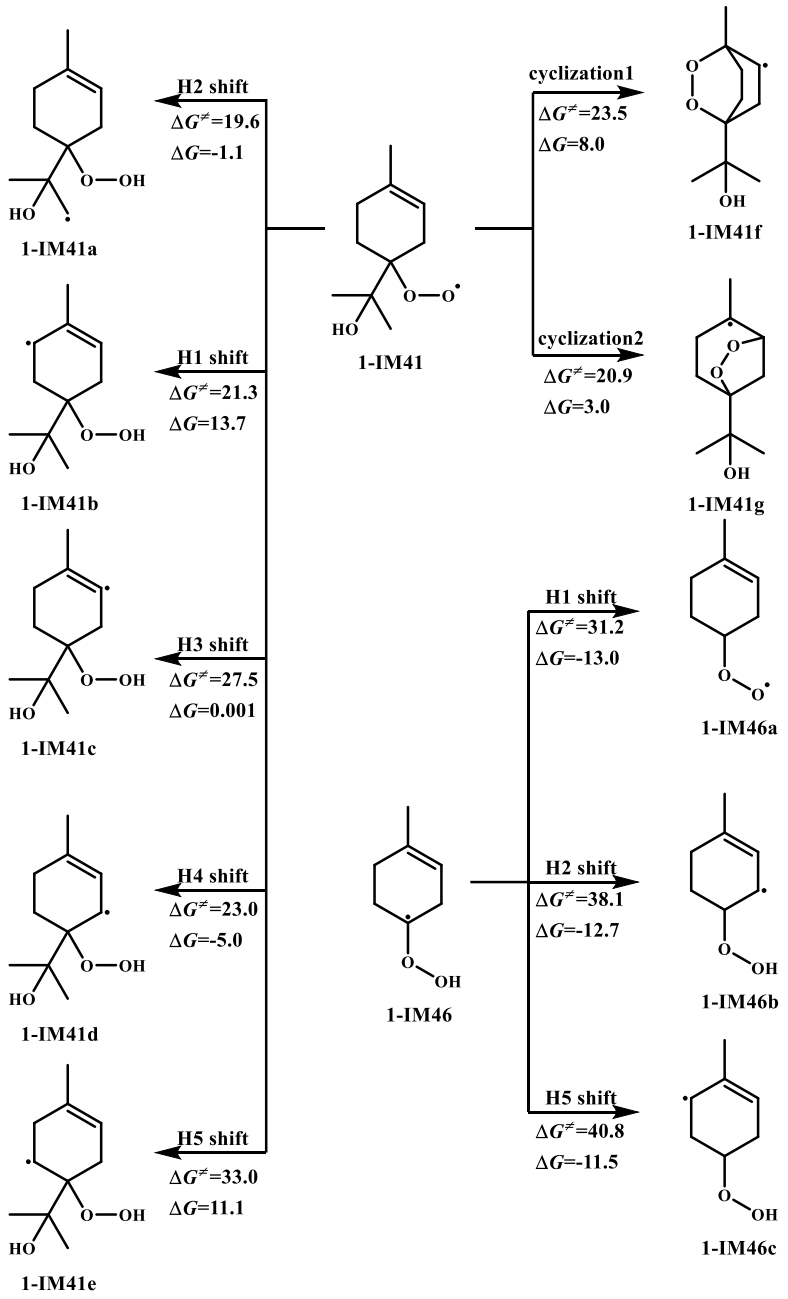

Figure S5. The H atom shift and cyclization reactions of 1-IM41 and 1-IM46 (unit in kcalmol^{-1})

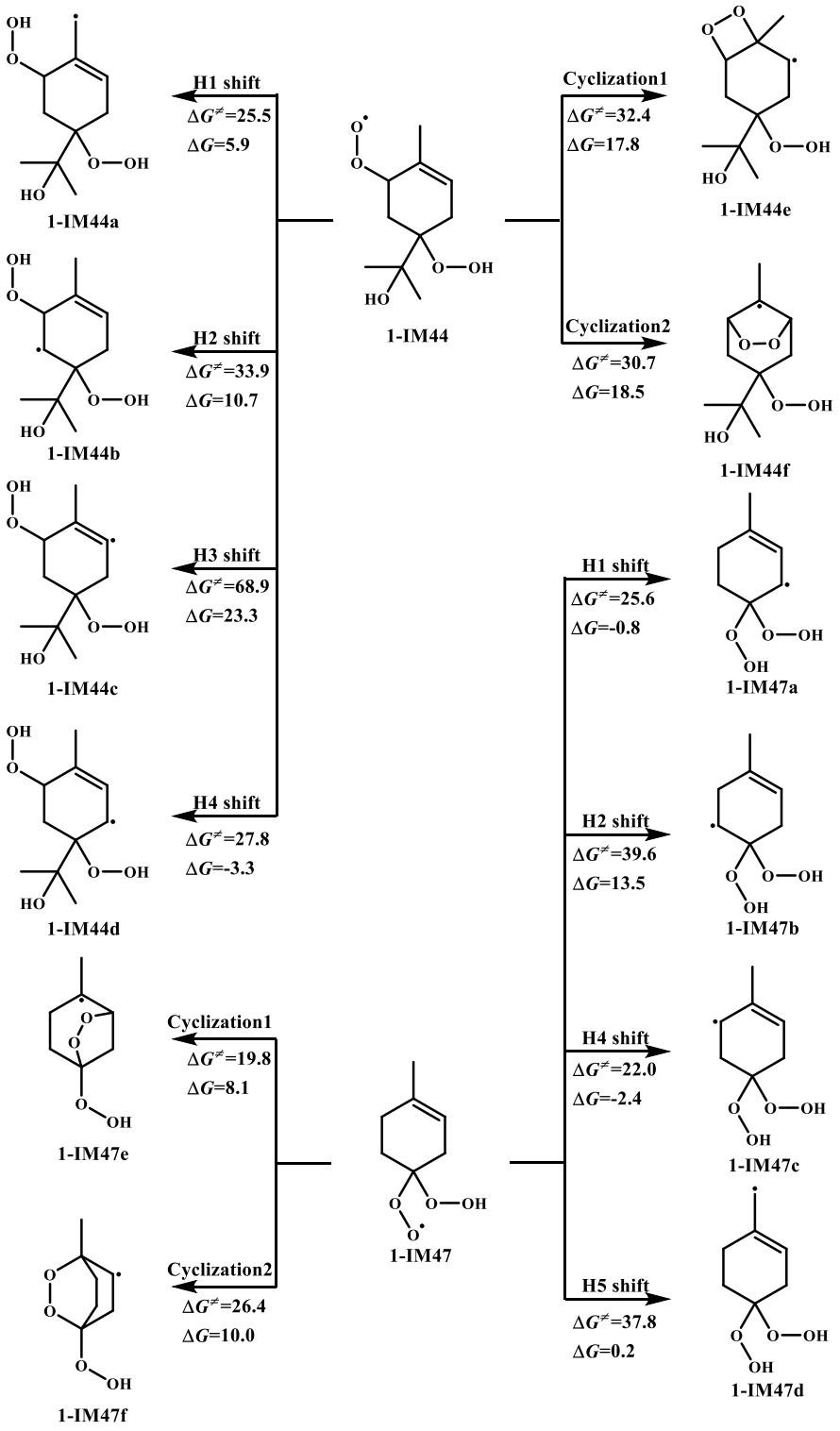

Figure S6. The H atom shift and cyclization reactions of 1-IM44 and 1-IM47 (unit in kcal mol^{-1})

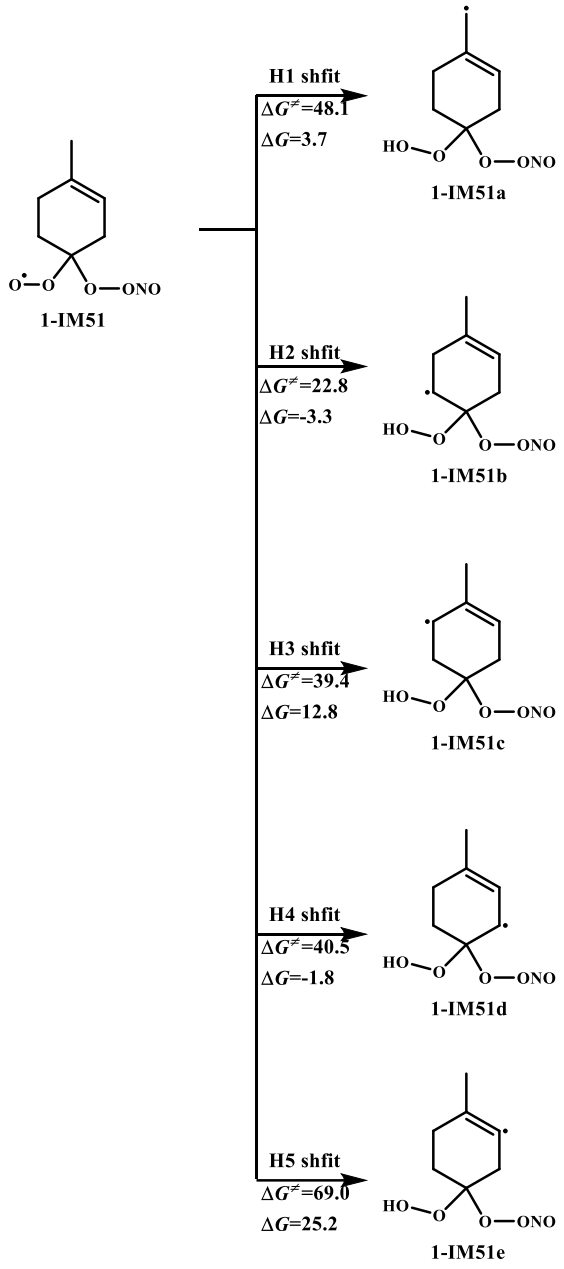

Figure S7. The H atom shift and cyclization reactions of 1-IM50 (unit in kcal mol^{-1})

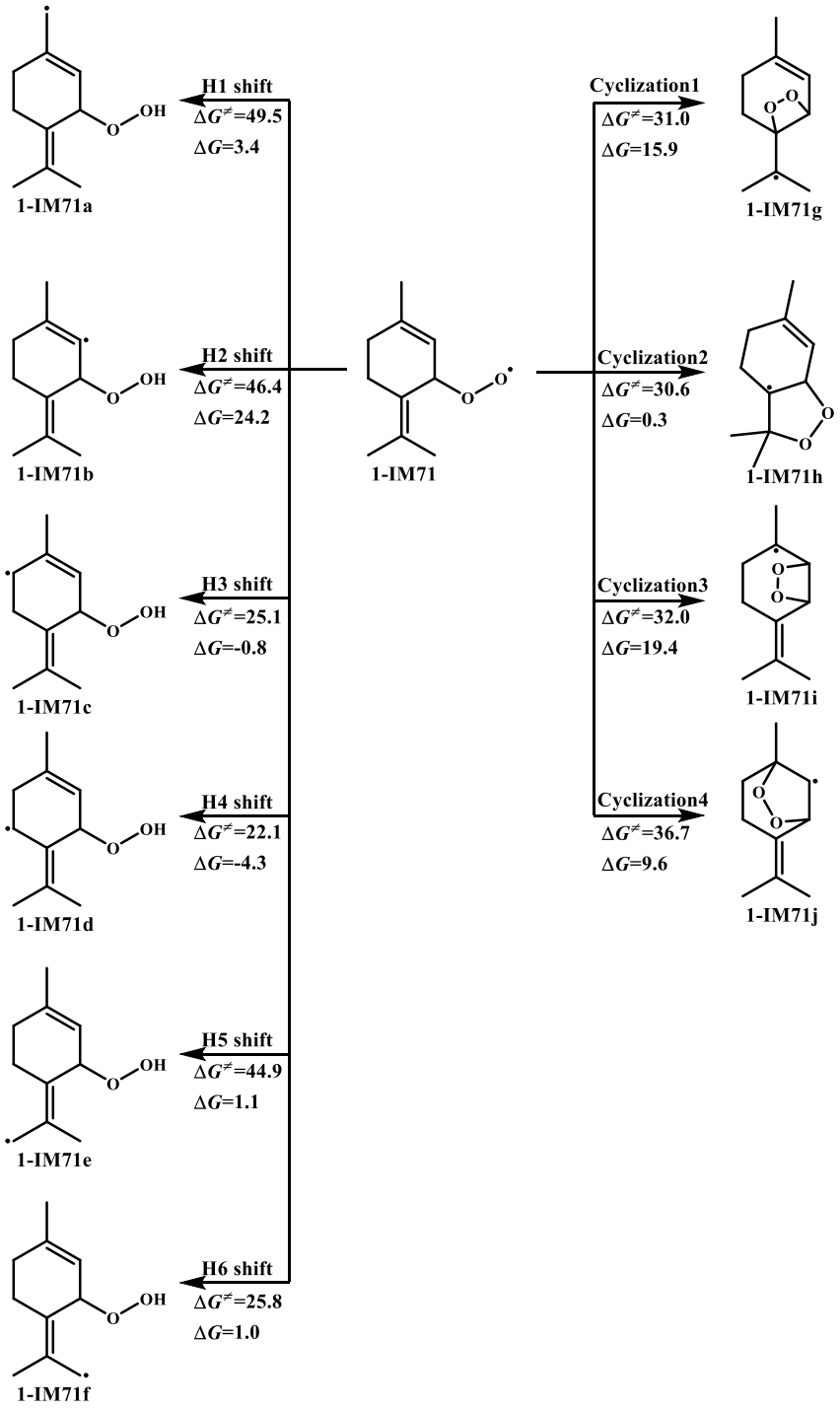

Figure S8. The H atom shift and cyclization reactions of 1-IM71 (unit in kcal mol^{-1})

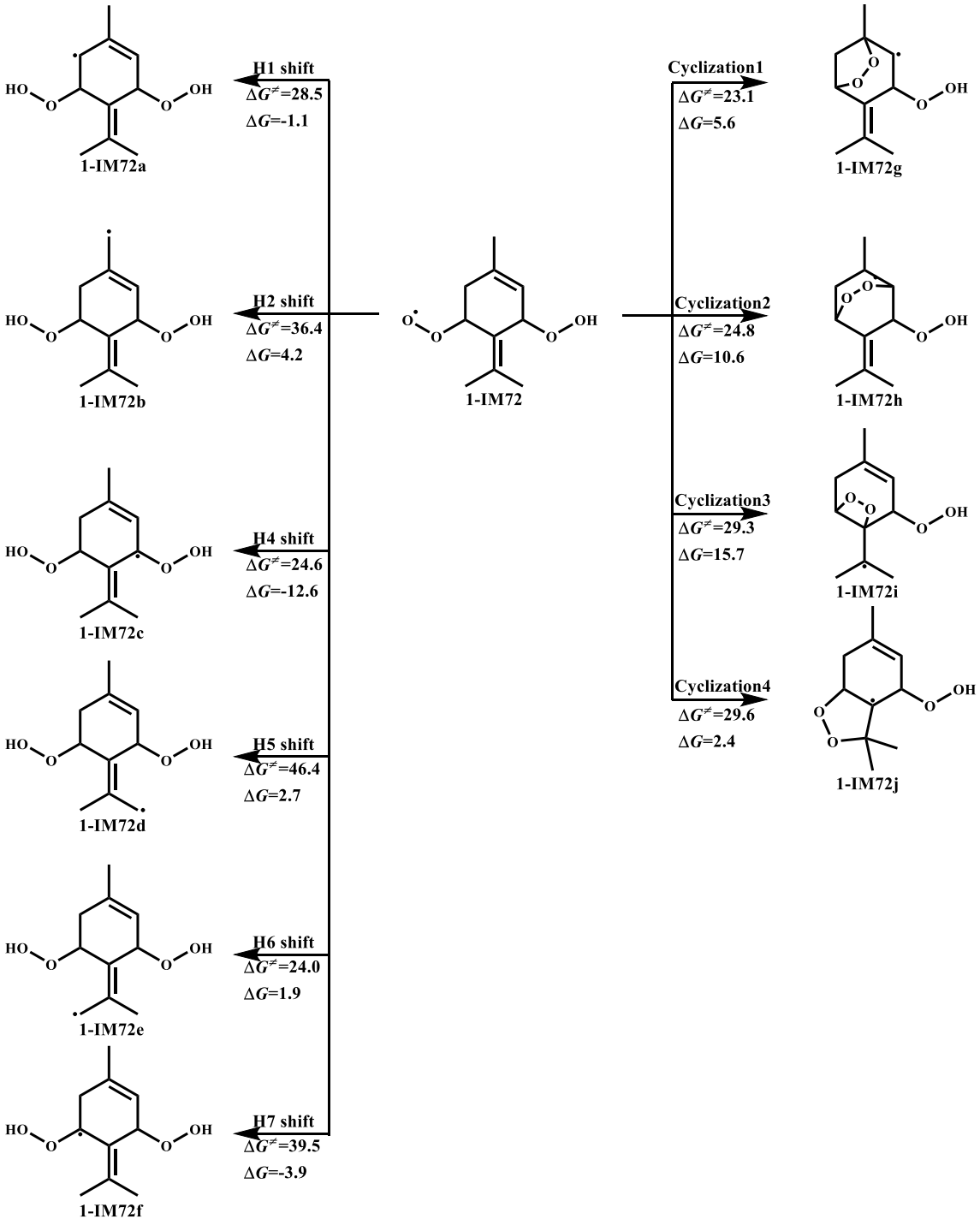

Figure S9. The H atom shift and cyclization reactions of 1-IM72 (unit in kcal mol^{-1})

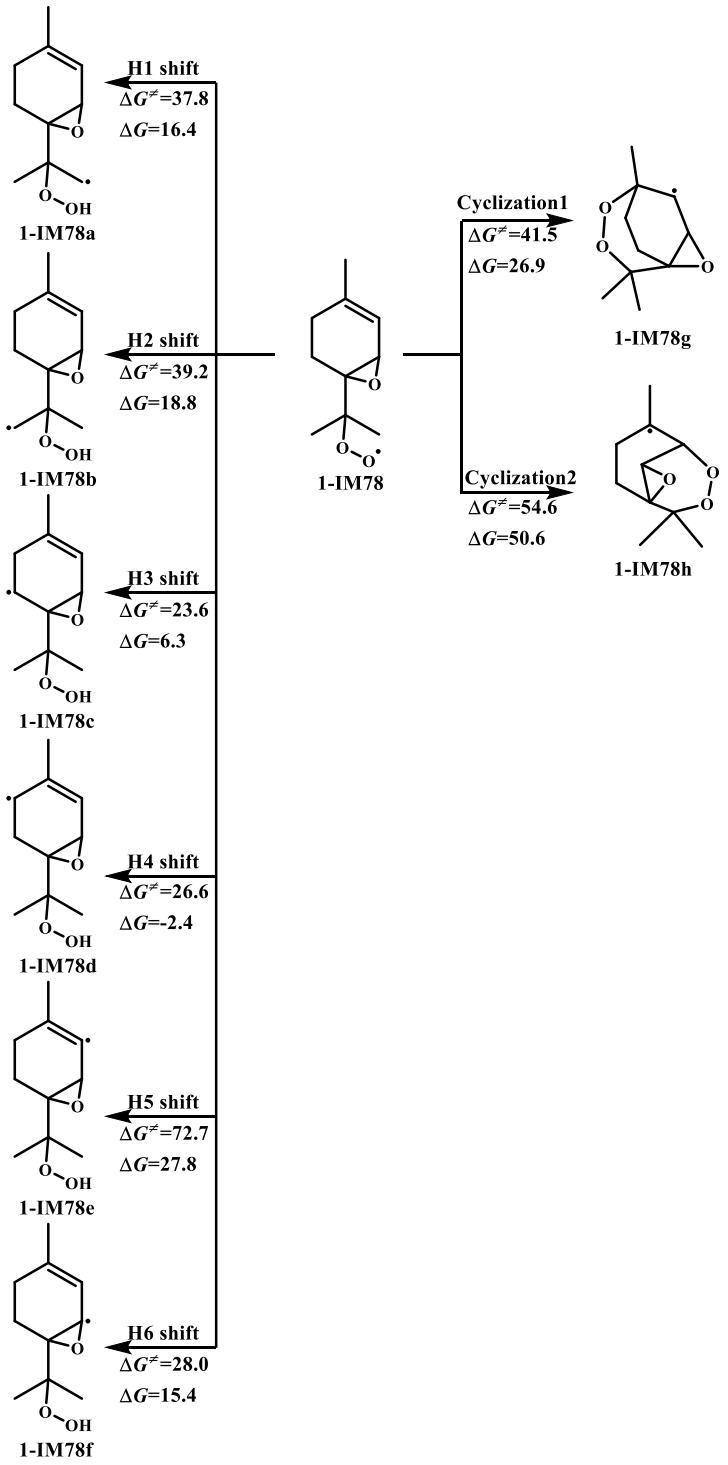

Figure S10. The H atom shift and cyclization reactions of 1-IM78 (unit in kcal mol^{-1})

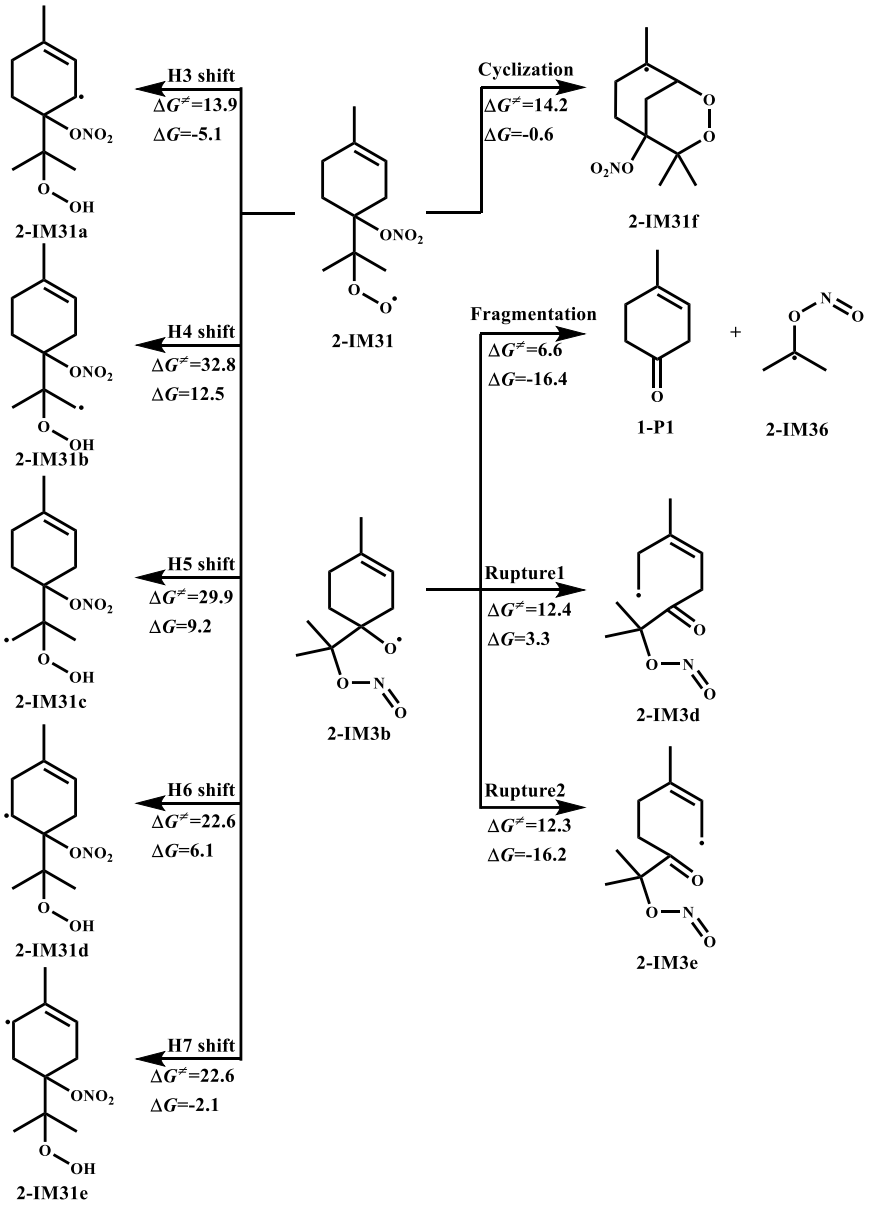

Figure S11. The subsequent reactions of 2-IM31 and 2-IM3b (unit in kcal mol^{-1})

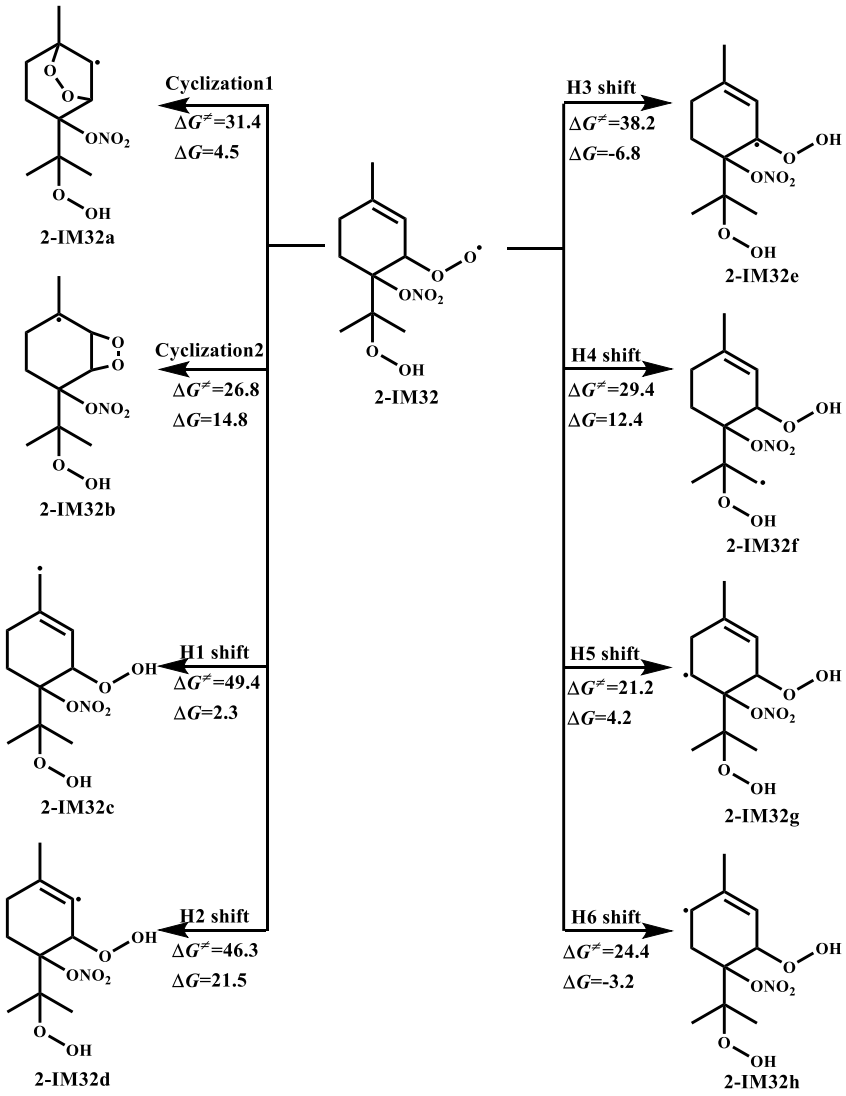

Figure S12. The H atom shift and cyclization reactions of 2-IM32 (unit in kcal mol^{-1})

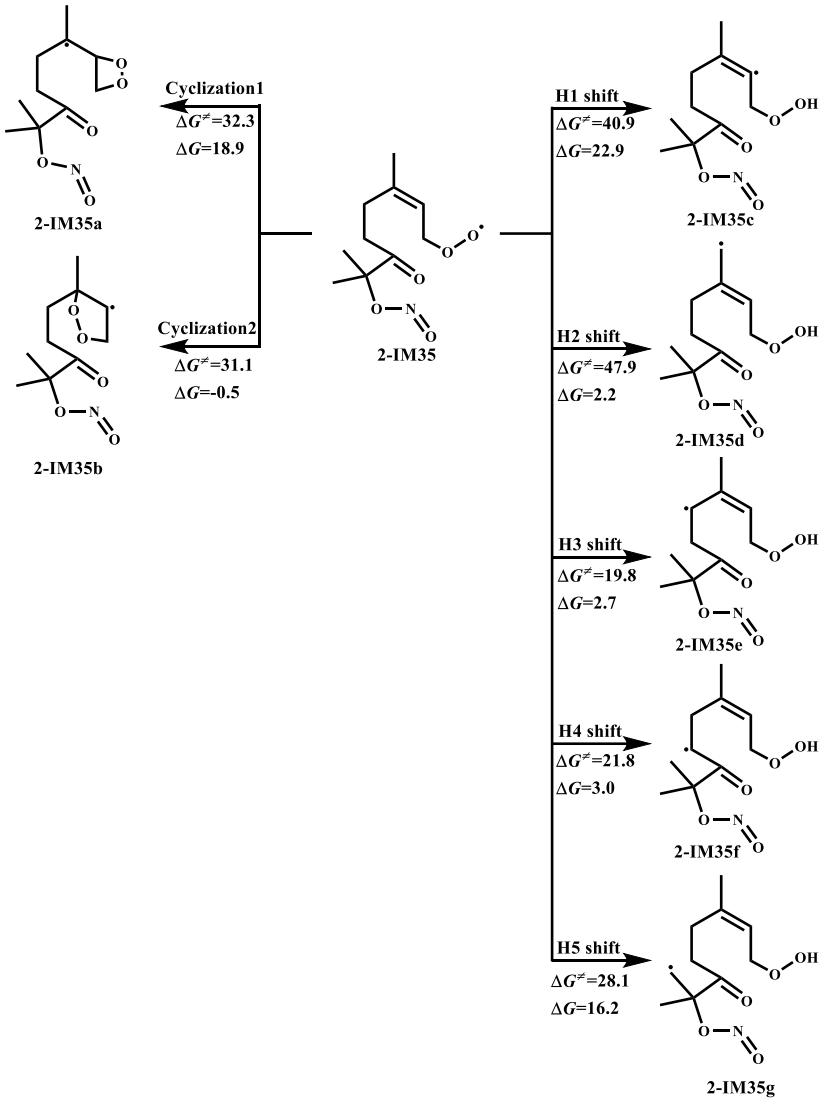

Figure S13. The H atom shift and cyclization reactions of 2-IM35 (unit in kcal mol^{-1})

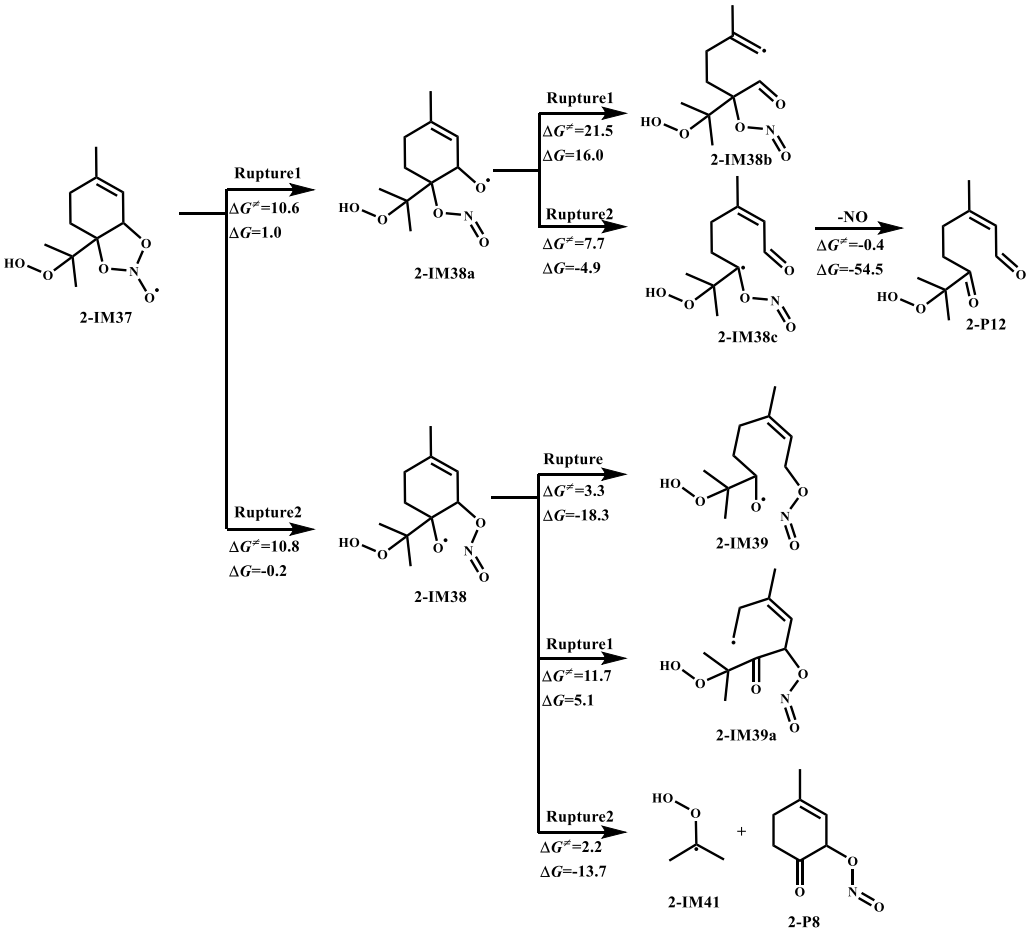

Figure S14. The subsequent reactions of 2-IM37 (unit in kcal mol^{-1})

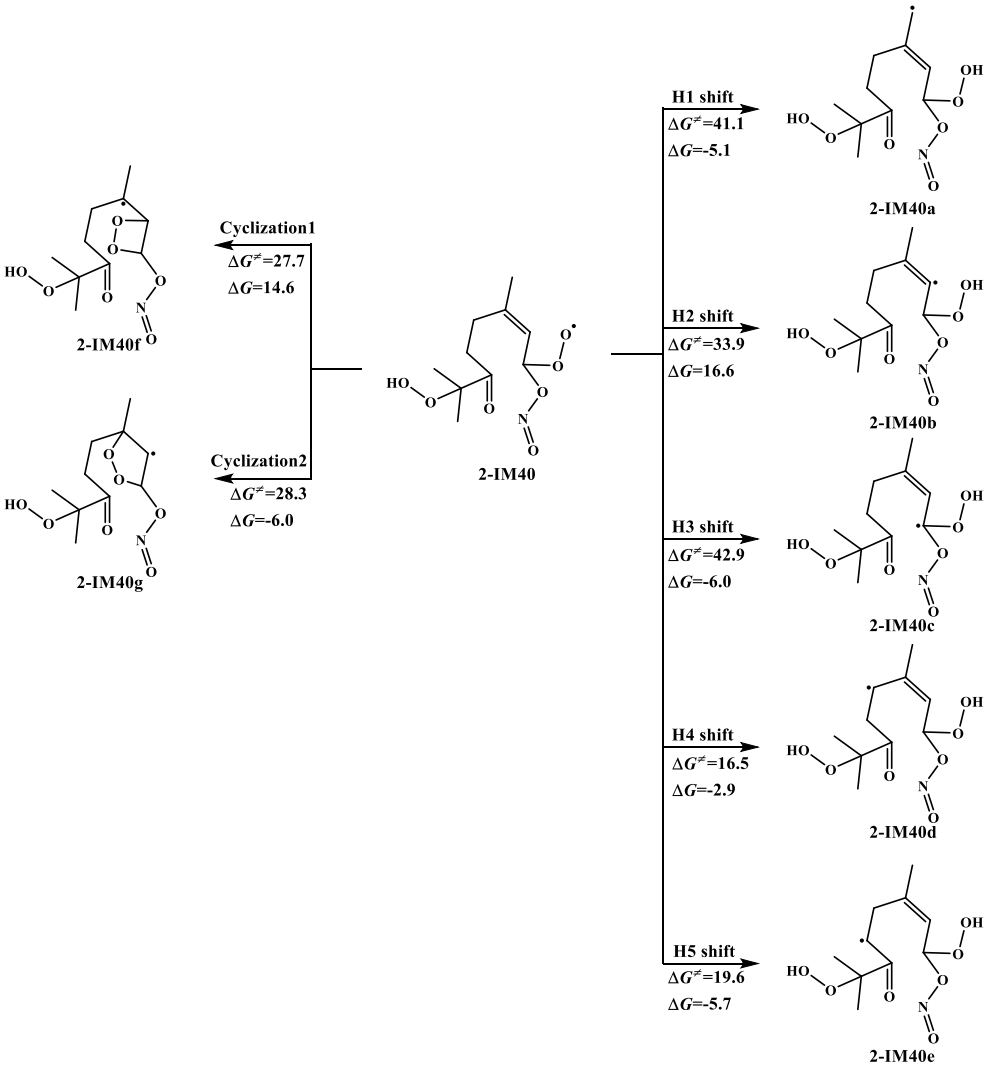

Figure S15. The H atom shift and cyclization reactions of 2-IM40 (unit in kcal mol^{-1})

S4 Summary of the Reactions Involved in the Zero-Dimensional Chemical Model

Table S1. The subsequent reactions of 1-IM4 and the rate constant of the rate-determining step.

Reactions	Rate constants	Reference
1-IM4 → 1-IM41a	3.72×10^{-1} s^{-1}	This Study
1-IM4 → 1-IM42	9.0×10^{-12} cm^3 $molecule^{-1}$ s^{-1}	Atkinson and Arey[4]
1-IM4 → 1-IM43	1.7×10^{-11} cm^3 $molecule^{-1}$ s^{-1}	Boyd et al.[5]
1-IM42→ 1-IM49	1.7×10^{-8} s^{-1}	This Study
1-IM49 → 1-IM51	6.0×10^{-12} cm^3 $molecule^{-1}$ s^{-1}	Wang and Wang[6], Wu et al.[7]
1-IM51 → 1-P12	1.7×10^{-11} cm^3 $molecule^{-1}$ s^{-1}	Boyd et al.[5]
1-IM51 → 1-IM51b	1.14×10^{-3} s^{-1}	This Study
1-IM51b → 1-P21	1.7×10^{-11} cm^3 $molecule^{-1}$ s^{-1}	Boyd et al.[5]
1-IM49 → 1-P1 + 1-P2	1.19×10^{8} s^{-1}	This Study
1-IM43 → 1-IM45	8.41×10^{-8} s^{-1}	This Study
1-IM45 → 1-IM47	6.0×10^{-12} cm^3 $molecule^{-1}$ s^{-1}	Wang and Wang[6], Wu et al.[7]
1-IM45 → 1-P1 + 1-P2	2.3×10^{8} s^{-1}	This Study
1-IM41a → 1-P9	9.0×10^{-12} cm^3 $molecule^{-1}$ s^{-1}	Atkinson and Arey[4]
1-IM41a → 1-P3	1.7×10^{-11} cm^3 $molecule^{-1}$ s^{-1}	Boyd et al.[5]
1-IM47 → 1-IM47c	5.55×10^{-3} s^{-1}	This study
1-IM47 → 1-P14	1.7×10^{-11} cm^3 $molecule^{-1}$ s^{-1}	Boyd et al.[5]
1-IM47c → 1-P4	1.7×10^{-11} cm^3 $molecule^{-1}$ s^{-1}	Boyd et al.[5]

Table S2. The subsequent reactions of 1-IM7 and the rate constant of the rate-determining step.

Reactions	Rate constants	Reference
1-IM7 → 1-IM74	1.7×10^{-11} cm^3 $molecule^{-1}$ s^{-1}	Boyd et al.[5]
1-IM7 → 1-IM76	9.0×10^{-12} cm^3 $molecule^{-1}$ s^{-1}	Atkinson and Arey[4]
1-IM7 → 1-IM71d	3.66×10^{-3} s^{-1}	This study
1-IM74 → 1-IM75	4.45×10^{-4} s^{-1}	This study
1-IM75 → 1-P7	5.93×10^{12} s^{-1}	This study
1-IM76 → 1-IM77	1.18×10^{-9} s^{-1}	This study
1-IM77 → 1-IM78	6.0×10^{-12} cm^3 $molecule^{-1}$ s^{-1}	Wang and Wang[6], Wu et al.[7]
1-IM78 → 1-P8	1.7×10^{-11} cm^3 $molecule^{-1}$ s^{-1}	Boyd et al.[5]
1-IM78 → 1-P11	9.0×10^{-12} cm^3 $molecule^{-1}$ s^{-1}	Atkinson and Arey[4]
1-IM78 → 1-IM78d	2.15×10^{-6} s^{-1}	This study
1-IM78d → 1-IM79	6.0×10^{-12} cm^3 $molecule^{-1}$ s^{-1}	Wang and Wang[6], Wu et al.[6]
1-IM79 → 1-P15	9.0×10^{-12} cm^3 $molecule^{-1}$ s^{-1}	Atkinson and Arey[4]
1-IM79 → 1-P16	1.10×10^{-11} cm^3 $molecule^{-1}$ s^{-1}	Saunders et al.[8]
1-IM79 → 1-P13	1.7×10^{-11} cm^3 $molecule^{-1}$ s^{-1}	Boyd et al.[5]
1-IM71d → 1-IM72	6.0×10^{-12} cm^3 $molecule^{-1}$ s^{-1}	Wang and Wang[6],Wu et al.[7]
1-IM72 → 1-P18	1.10×10^{-11} cm^3 $molecule^{-1}$ s^{-1}	Saunders et al.[8]
1-IM72 → 1-P5	1.7×10^{-11} cm^3 $molecule^{-1}$ s^{-1}	Boyd et al.[5]
1-IM72 → 1-IM72c	2.8×10^{-5} s^{-1}	This study
1-IM72c → 1-IM73	6.0×10^{-12} cm^3 $molecule^{-1}$ s^{-1}	Wang and Wang[6], Wu et al.[7]
1-IM73 → 1-P20	1.10×10^{-11} cm^3 $molecule^{-1}$ s^{-1}	Saunders et al.[8]
1-IM73 → 1-P19	9.0×10^{-12} cm^3 $molecule^{-1}$ s^{-1}	Atkinson and Arey[4]
1-IM73 → 1-P6	1.7×10^{-11} cm^3 $molecule^{-1}$ s^{-1}	Boyd et al.[5]
1-IM72 → 1-P17	9.0×10^{-12} cm^3 $molecule^{-1}$ s^{-1}	Atkinson and Arey[4]

Table S3. The subsequent reactions of 2-IM3 and the rate constant of the rate-determining step.

Reactions	Rate constants	Reference
2-IM3 → 2-IM3a	2.71×10 s^{-1}	This study
2-IM3a → 1-P2 + 1-P1 + NO	7.45×10^{5} s^{-1}	This study
2-IM3a → 1-P2 + 1-P1 + NO	4.28×10^{4} s^{-1}	This study
2-IM3a → 2-IM3e	7.28×10^{3} s^{-1}	This study
2-IM3e → 2-IM35	6.0×10^{-12} cm^{3} $molecule^{-1}$ s^{-1}	Wang and Wang[6],Wu et al.[7]
2-IM35 → 2-P5 + O_2	1.7×10^{-11} cm^{3} $molecule^{-1}$ s^{-1}	Boyd et al.[5]
2-IM3 → 2-IM31f	3.42×10^{2} s^{-1}	This study
2-IM3 → 2-IM31a	3.83×10^{3} s^{-1}	This study
2-IM3 →2-P4+O_2	1.7×10^{-11} cm^{3} $molecule^{-1}$ s^{-1}	Boyd et al.[5]
2-IM3 →2-P2	9.0×10^{-12} cm^{3} $molecule^{-1}$ s^{-1}	Atkinson and Arey[4]
2-IM31f → 2-P3+1-P2+ NO_2	5.29×10^{-8} s^{-1}	This study
2-IM31f → 2-P14+O_2	1.7×10^{-11} cm^{3} $molecule^{-1}$ s^{-1}	Boyd et al.[5]
2-IM31f → 2-P15	9.0×10^{-12} cm^{3} $molecule^{-1}$ s^{-1}	Atkinson and Arey[4]
2-IM31f → 2-P16	1.10×10^{-11} cm^{3} $molecule^{-1}$ s^{-1}	Saunders et al.[8]
2-IM31a →2-P9	9.0×10^{-12} cm^{3} $molecule^{-1}$ s^{-1}	Atkinson and Arey[4]
2-IM31a → 2-P11 + O_2	1.7×10^{-11} cm^{3} $molecule^{-1}$ s^{-1}	Boyd et al.[5]
2-IM31a → 2-P10	1.10×10^{-11} cm^{3} $molecule^{-1}$ s^{-1}	Saunders et al[8]
2-IM31a → 2-IM32h	6.78×10^{-5} s^{-1}	This study
2-IM31a →2-IM37	1.17×10^{2} s^{-1}	This study
2-IM32h → 2-P6 + O_2	1.7×10^{-11} cm^{3} $molecule^{-1}$ s^{-1}	Boyd et al.[5]
2-IM37 → 2-IM40	8.21×10^{4} s^{-1}	This study
2-IM37 → 2-P12	8.21×10^{4} s^{-1}	This study
2-IM37 → 2-P8 + 1-P2 + OH	8.21×10^{4} s^{-1}	This study
2-IM40 → 2-P17	9.0×10^{-12} cm^{3} $molecule^{-1}$ s^{-1}	Atkinson and Arey[4]
2-IM40 → 2-P18	1.10×10^{-11} cm^{3} $molecule^{-1}$ s^{-1}	Saunders et al.[8]
2-IM40 → 2-P13	1.7×10^{-11} cm^{3} $molecule^{-1}$ s^{-1}	Boyd et al.[5]
2-IM40 → 2-IM43	4.43×10 s^{-1}	This study
2-IM43 → 2-P19	9.0×10^{-12} cm^{3} $molecule^{-1}$ s^{-1}	Atkinson and Arey[4]
2-IM43 → 2-P20	1.10×10^{-11} cm^{3} $molecule^{-1}$ s^{-1}	Saunders et al.[8]
2-IM43 → 2-P7	1.7×10^{-11} cm^{3} $molecule^{-1}$ s^{-1}	Boyd et al.[5]

S5 The Time-Dependent Fractional Yield of the Major Products from the Oxidation of OH-Ter-R• (1-IM4 and 1-IM7)

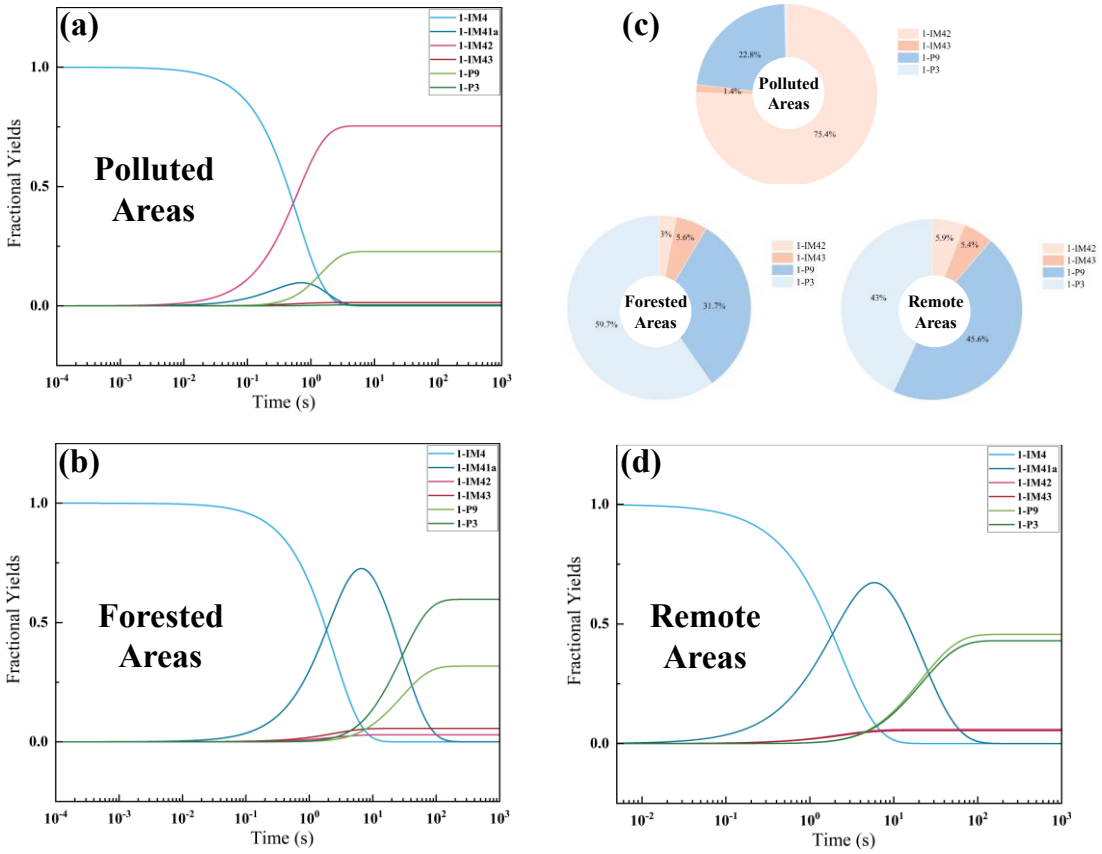

Figure S16. The modeled time-dependent fractional yields of important species from the further reactions of OH-Ter-R• (1-IM4) under the atmospheric conditions of polluted areas (a), forested areas (b), remote areas (d) (Species with yields <0.1% excluded).

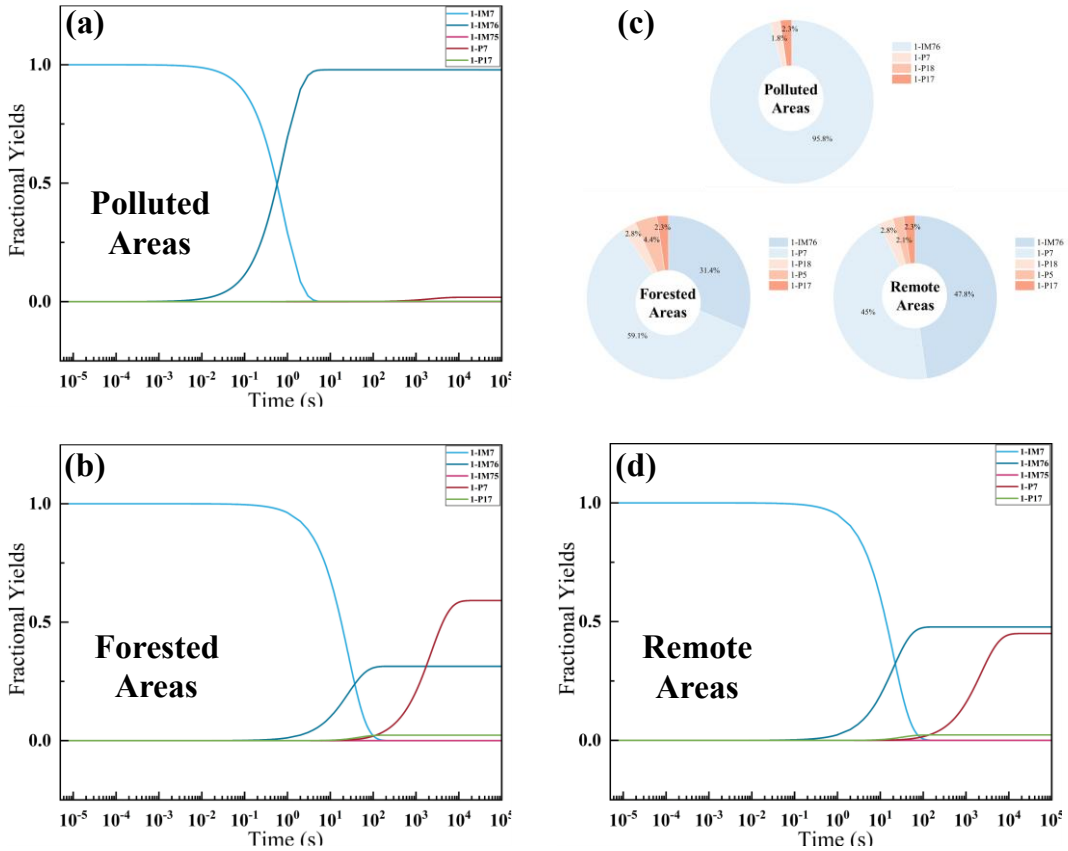

Figure S17. The modeled time-dependent fractional yields of important species from the further reactions of OH-Ter-R• (1-IM7) under the atmospheric conditions of polluted areas (a), forested areas (b), remote areas (d) (Species with yields <0.1% excluded).

S6 Main Products of the Atmospheric Oxidation of the OH-Ter-R• (1-IM4 and 1-IM7) and NO_3-Ter-R• (2-IM3)

Table S4. Structural and nomenclatural data for major products reported in previous studies.

Product structure	Chemical formula, Systematic name	Reference
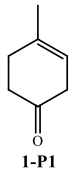 1-P1	$C_7H_{10}O$, 4-methylcyclohex-3-en-1-one	Fouqueau et al.[9], Hakola et al.[10], Orlando et al.[11], Reissell et al.[12]
 1-P2	$C_{10}H_{18}O_5$, C_3H_6O, propan-2-one	Fouqueau et al.[9], Hakola et al.[10], Orlando et al.[11], Reissell et al.[12]
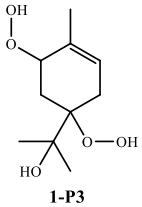 1-P3	$C_7H_{12}O_6$, 2-(1,5-dihydroperoxy-4-methylcyclohex-3-en-1-yl)propan-2-ol	Guo et al.[13], Zheng et al.[14]
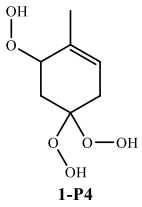 1-P4	$C_7H_{12}O_6$, 4,4,6-trihydroperoxy-1-methylcyclohex-1-ene	
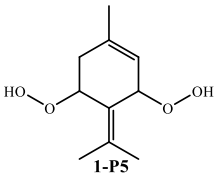 1-P5	$C_{10}H_{16}O_4$, 3,5-dihydroperoxy-1-methyl-4-(propan-2-ylidene)cyclohex-1-ene	Guo et al.[13], Zheng et al.[14]
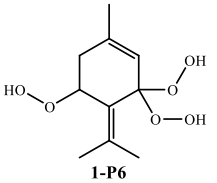 1-P6	$C_{10}H_{16}O_6$, 3,3,5-trihydroperoxy-1-methyl-4-(propan-2-ylidene)cyclohex-1-ene	Luo et al.[15], Zheng et al.[14]
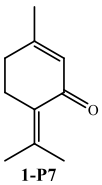 1-P7	$C_{10}H_{14}O$, 3-methyl-6-(propan-2-ylidene)cyclohex-2-en-1-one	

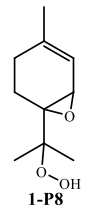 **1-P8**	$C_{10}H_{16}O_3$, 6-(2-hydroperoxypropan-2-yl)-3-methyl-7-oxabicyclo[4.1.0]hept-2-ene	Fouqueau et al.[9]
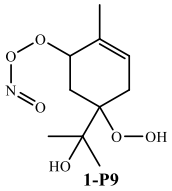 **1-P9**	$C_{10}H_{17}O_6$, 5-hydroperoxy-5-(2-hydroxypropan-2-yl)-2-methylcyclohex-2-en-1-yl nitroperoxoite	Luo et al.[15], Zheng et al.[14]
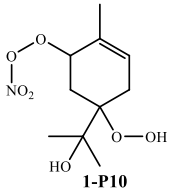 **1-P10**	$C_{10}H_{17}NO_7$, 5-hydroperoxy-5-(2-hydroxypropan-2-yl)-2-methylcyclohex-2-en-1-yl) nitroperoxoate	Guo et al.[13], Luo et al.[15], Massoli et al.[16], Zheng et al.[14]
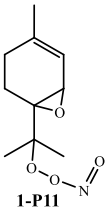 **1-P11**	$C_{10}H_{15}NO_4$, 2-(4-methyl-7-oxabicyclo[4.1.0]hept-4-en-1-yl)propan-2-yl nitroperoxoite	Fouqueau et al.[9]
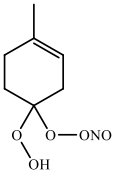 **1-P12**	$C_7H_{12}NO_5$, 1-hydroperoxy-4-methylcyclohex-3-en-1-yl nitroperoxoite	
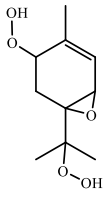 **1-P13**	$C_{10}H_{16}O_5$, 4-hydroperoxy-6-(2-hydroperoxypropan-2-yl)-3-methyl-7-oxabicyclo[4.1.0]hept-2-ene	Luo et al.[15], Zheng et al.[14]
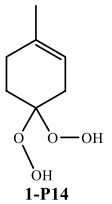 **1-P14**	$C_7H_{12}O_4$, 4,4-dihydroperoxy-1-methylcyclohex-1-ene	
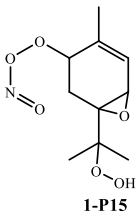 **1-P15**	$C_{10}H_{15}NO_6$, 1-(2-hydroperoxypropan-2-yl)-4-methyl-7-oxabicyclo[4.1.0]hept-4-en-3-yl nitroperoxoite	Fouqueau et al.[9], Liu et al.[17]

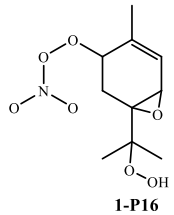 1-P16	$C_{10}H_{15}NO_7$, N-((1-(2-hydroperoxypropan-2-yl)-4-methyl-7-oxabicyclo[4.1.0]hept-4-en-3-yl)peroxy)-N-(l1-oxidaneyl)hydroxylamine	Fouqueau et al.[9], Guo et al.[13], Liu et al.[17], Luo et al.[15], Zheng et al.[14]
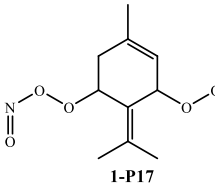 1-P17	$C_{10}H_{15}NO_5$, 5-hydroperoxy-3-methyl-6-(propan-2-ylidene)cyclohex-3-en-1-yl nitroperoxoite	Fouqueau et al.[9]
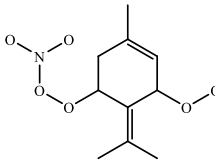 1-P18	$C_{10}H_{15}NO_6$, N-((5-hydroperoxy-3-methyl-6-(propan-2-ylidene)cyclohex-3-en-1-yl)peroxy)-N-(l1-oxidaneyl)hydroxylamine	Fouqueau et al.[9], Liu et al.[17],Massoli et al.[16], Shen et al.[18], Zheng et al.[14]
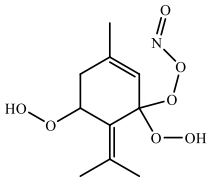 1-P19	$C_{10}H_{15}NO_7$, 1,5-dihydroperoxy-3-methyl-6-(propan-2-ylidene)cyclohex-2-en-1-yl nitroperoxoite	Fouqueau et al.[9], Guo et al.[13],Liu et al.[17],Luo et al.[15],Zheng et al.[14]
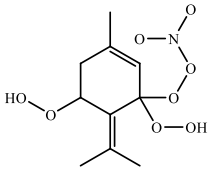 1-P20	$C_{10}H_{15}NO_8$, N-((1,5-dihydroperoxy-3-methyl-6-(propan-2-ylidene)cyclohex-2-en-1-yl)peroxy)-N-(l1-oxidaneyl)hydroxylamine	Guo et al.[13],Luo et al.[15],Massoli et al.[16],Zheng et al.[14]
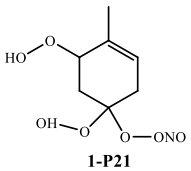 1-P21	$C_7H_{11}NO_7$, 1,5-dihydroperoxy-4-methylcyclohex-3-en-1-yl nitroperoxoite	
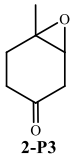 2-P3	$C_7H_{10}O_2$, 6-methyl-7-oxabicyclo[4.1.0]heptan-3-one	Fouqueau et al.[9]
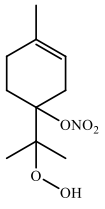 2-P4	$C_{10}H_{17}NO_5$, 1-(2-hydroperoxypropan-2-yl)-4-methylcyclohex-3-en-1-yl nitrate	Luo et al.[15], Zheng et al.[14]

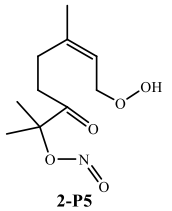 2-P5	$C_{10}H_{17}NO_5$, (Z)-8-hydroperoxy-2,6-dimethyl-3-oxooct-6-en-2-yl nitrite	Luo et al.[15], Zheng et al.[14]
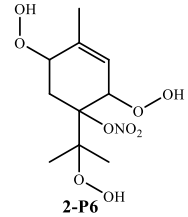 2-P6	$C_{10}H_{17}NO_9$, 2,5-dihydroperoxy-1-(2-hydroperoxypropan-2-yl)-4-methylcyclohex-3-en-1-yl nitrate	Guo et al.[13], Luo et al.[15], Zheng et al.[14]
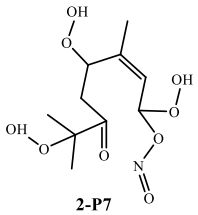 2-P7	$C_{10}H_{17}NO_9$, (Z)-1,4,7-trihydroperoxy-3,7-dimethyl-6-oxooct-2-en-1-yl nitrite	Guo et al.[13], Luo et al.[15], Zheng et al.[14]
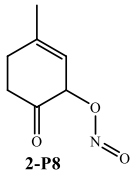 2-P8	$C_7H_9NO_3$, 3-methyl-6-oxocyclohex-2-en-1-yl nitrite	
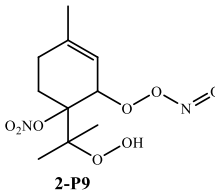 2-P9	$C_{10}H_{16}N_2O_8$, 1-(2-hydroperoxypropan-2-yl)-4-methyl-2-(nitrosoperoxy)cyclohex-3-en-1-yl nitrate	Liu et al.[19], Liu et al.[17], Shen et al.[18], Zheng et al.[14]
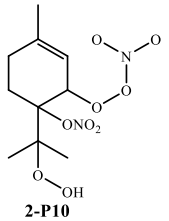 2-P10	$C_{10}H_{16}N_2O_9$, 2-((di(l1-oxidaneyl)amino)peroxy)-1-(2-hydroperoxypropan-2-yl)-4-methylcyclohex-3-en-1-yl nitrate	Guo et al.[13], Liu et al.[17], Liu et al.[19], Massoli et al.[16], Zheng et al.[14]
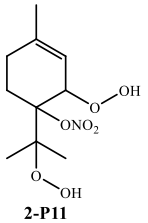 2-P11	$C_{10}H_{17}NO_7$, 2-hydroperoxy-1-(2-hydroperoxypropan-2-yl)-4-methylcyclohex-3-en-1-yl nitrate	Guo et al.[13], Luo et al.[15], Massoli et al.[16], Zheng et al.[14]

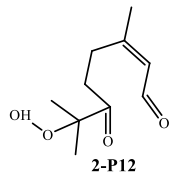 2-P12	$C_{10}H_{16}O_4$, (Z)-7-hydroperoxy-3,7-dimethyl-6-oxooct-2-enal	Guo et al.[13], Zheng et al.[14]
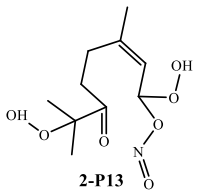 2-P13	$C_{10}H_{17}NO_7$, (Z)-1,7-dihydroperoxy-3,7-dimethyl-6-oxooct-2-en-1-yl nitrite	Guo et al.[13], Luo et al.[15], Massoli et al.[16], Zheng et al.[14]
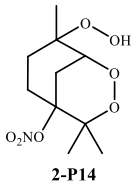 2-P14	$C_{10}H_{17}NO_7$, 8-hydroperoxy-4,4,8-trimethyl-2,3-dioxabicyclo[3.3.1]nonan-5-yl nitrate	Guo et al.[13], Luo et al.[15], Massoli et al.[16], Zheng et al.[14]
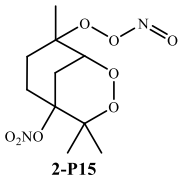 2-P15	$C_{10}H_{16}N_2O_8$, 4,4,8-trimethyl-8-(nitrosoperoxy)-2,3-dioxabicyclo[3.3.1]nonan-5-yl nitrate	Liu et al.[19],Liu et al.[17],Shen et al.[18],Zheng et al.[14]
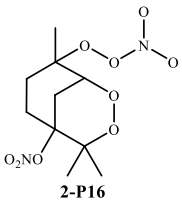 2-P16	$C_{10}H_{16}N_2O_9$, 8-((di(l1-oxidaneyl)amino)peroxy)-4,4,8-trimethyl-2,3-dioxabicyclo[3.3.1]nonan-5-yl nitrate	Guo et al.[13],Liu et al.[17],Massoli et al.[16],Zheng et al.[14]
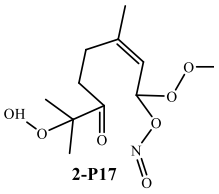 2-P17	$C_{10}H_{16}N_2O_8$, (Z)-7-hydroperoxy-3,7-dimethyl-1-(nitrosoperoxy)-6-oxooct-2-en-1-yl nitrite	Liu et al.[17],Shen et al.[18],Zheng et al.[14]
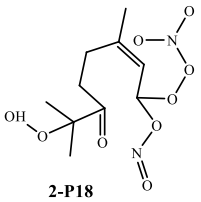 2-P18	$C_{10}H_{16}N_2O_9$, (Z)-1-((di(l1-oxidaneyl)amino)peroxy)-7-hydroperoxy-3,7-dimethyl-6-oxooct-2-en-1-yl nitrite	Guo et al.[13],Liu et al.[17],Liu et al.[19],Massoli et al.[16],Zheng et al.[14]
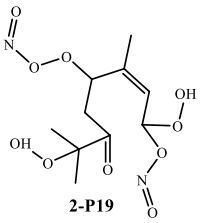 2-P19	$C_{10}H_{16}N_2O_{10}$, (Z)-1,7-dihydroperoxy-3,7-dimethyl-4-(nitrosoperoxy)-6-oxooct-2-en-1-yl nitrite	Guo et al.[13],Luo et al.[15],Zheng et al.[14]

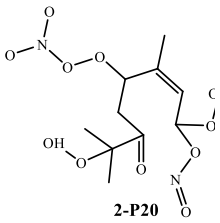 2-P20	$C_{10}H_{16}N_2O_{11}$, (Z)-4-((di(l1-oxidaneyl)amino)peroxy)-1,7-dihydroperoxy-3,7-dimethyl-6-oxooct-2-en-1-yl nitrite	Zheng et al.[14]

References

1. Mohr, C.; Thornton, J. A.; Heitto, A.; Lopez-Hilfiker, F. D.; Lutz, A.; Riipinen, I.; Hong, J.; Donahue, N. M.; Hallquist, M.; Petäjä, T.; Kulmala, M.; Yli-Juuti, T., Molecular identification of organic vapors driving atmospheric nanoparticle growth. *Nature Communications* **2019,** *10* (1), 4442.
2. Tröstl, J.; Chuang, W. K.; Gordon, H.; Heinritzi, M.; Yan, C.; Molteni, U.; Ahlm, L.; Frege, C.; Bianchi, F.; Wagner, R.; Simon, M.; Lehtipalo, K.; Williamson, C.; Craven, J. S.; Duplissy, J.; Adamov, A.; Almeida, J.; Bernhammer, A.-K.; Breitenlechner, M.; Brilke, S.; Dias, A.; Ehrhart, S.; Flagan, R. C.; Franchin, A.; Fuchs, C.; Guida, R.; Gysel, M.; Hansel, A.; Hoyle, C. R.; Jokinen, T.; Junninen, H.; Kangasluoma, J.; Keskinen, H.; Kim, J.; Krapf, M.; Kürten, A.; Laaksonen, A.; Lawler, M.; Leiminger, M.; Mathot, S.; Möhler, O.; Nieminen, T.; Onnela, A.; Petäjä, T.; Piel, F. M.; Miettinen, P.; Rissanen, M. P.; Rondo, L.; Sarnela, N.; Schobesberger, S.; Sengupta, K.; Sipilä, M.; Smith, J. N.; Steiner, G.; Tomè, A.; Virtanen, A.; Wagner, A. C.; Weingartner, E.; Wimmer, D.; Winkler, P. M.; Ye, P.; Carslaw, K. S.; Curtius, J.; Dommen, J.; Kirkby, J.; Kulmala, M.; Riipinen, I.; Worsnop, D. R.; Donahue, N. M.; Baltensperger, U., The role of low-volatility organic compounds in initial particle growth in the atmosphere. *Nature* **2016,** *533* (7604), 527-531.
3. Donahue, N. M.; Kroll, J. H.; Pandis, S. N.; Robinson, A. L., A two-dimensional volatility basis set – Part 2: Diagnostics of organic-aerosol evolution. *Atmospheric Chemistry and Physics* **2012,** *12* (2), 615-634.
4. Atkinson, R.; Arey, J., Atmospheric Degradation of Volatile Organic Compounds. *Chemical Reviews* **2003,** *103* (12), 4605-4638.
5. Boyd, A. A.; Flaud, P.-M.; Daugey, N.; Lesclaux, R., Rate Constants for RO2 + HO2 Reactions Measured under a Large Excess of HO2. *The Journal of Physical Chemistry A* **2003,** *107* (6), 818-821.
6. Wang, S.; Wang, L., The atmospheric oxidation of dimethyl, diethyl, and diisopropyl ethers. The role of the intramolecular hydrogen shift in peroxy radicals. *Phys. Chem. Chem. Phys. (UK)* **2016,** *18* (11), 7707-7714.
7. Wu, R.; Wang, S.; Wang, L., New Mechanism for the Atmospheric Oxidation of Dimethyl Sulfide. The Importance of Intramolecular Hydrogen Shift in a CH_3SCH_2OO Radical. *The Journal of Physical Chemistry A* **2015,** *119* (1), 112-117.
8. Saunders, S. M.; Jenkin, M. E.; Derwent, R. G.; Pilling, M. J., Protocol for the development of the Master Chemical Mechanism, MCM v3 (Part A): tropospheric degradation of non-aromatic volatile organic compounds. *Atmospheric Chemistry and Physics* **2003,** *3* (1), 161-180.
9. Fouqueau, A.; Cirtog, M.; Cazaunau, M.; Pangui, E.; Doussin, J. F.; Picquet-Varrault, B., An experimental study of the reactivity of terpinolene and β-caryophyllene with the nitrate radical. *Atmospheric Chemistry and Physics* **2022,** *22* (10), 6411-6434.
10. Hakola, H.; Arey, J.; Aschmann, S. M.; Atkinson, R., Product formation from the gas-phase reactions of OH radicals and O3 with a series of monoterpenes. *Journal of Atmospheric Chemistry* **1994,** *18* (1), 75-102.
11. Orlando, J. J.; Nozière, B.; Tyndall, G. S.; Orzechowska, G. E.; Paulson, S. E.; Rudich, Y., Product studies of the OH- and ozone-initiated oxidation of some monoterpenes. *Journal of Geophysical Research-Atmospheres* **2000,** *105* (D9), 11561-11572.
12. Reissell, A.; Harry, C.; Aschmann, S. M.; Atkinson, R.; Arey, J., Formation of acetone from the OH radical- and O3-initiated reactions of a series of monoterpenes. *Journal of Geophysical Research-*

Atmospheres **1999,** *104* (D11), 13869-13879.
13. Guo, Y.; Yan, C.; Liu, Y.; Qiao, X.; Zheng, F.; Zhang, Y.; Zhou, Y.; Li, C.; Fan, X.; Lin, Z.; Feng, Z.; Zhang, Y.; Zheng, P.; Tian, L.; Nie, W.; Wang, Z.; Huang, D.; Daellenbach, K. R.; Yao, L.; Dada, L.; Bianchi, F.; Jiang, J.; Liu, Y.; Kerminen, V. M.; Kulmala, M., Seasonal variation in oxygenated organic molecules in urban Beijing and their contribution to secondary organic aerosol. *Atmospheric Chemistry and Physics* **2022,** *22* (15), 10077-10097.
14. Zheng, P.; Chen, Y.; Wang, Z.; Liu, Y.; Pu, W.; Yu, C.; Xia, M.; Xu, Y.; Guo, J.; Guo, Y.; Tian, L.; Qiao, X.; Huang, D. D.; Yan, C.; Nie, W.; Worsnop, D. R.; Lee, S.; Wang, T., Molecular Characterization of Oxygenated Organic Molecules and Their Dominating Roles in Particle Growth in Hong Kong. *Environmental Science & Technology* **2023,** *57* (20), 7764-7776.
15. Luo, H.; Vereecken, L.; Shen, H.; Kang, S.; Pullinen, I.; Hallquist, M.; Fuchs, H.; Wahner, A.; Kiendler-Scharr, A.; Mentel, T. F.; Zhao, D., Formation of highly oxygenated organic molecules from the oxidation of limonene by OH radical: significant contribution of H-abstraction pathway. *Atmospheric Chemistry and Physics* **2023,** *23* (13), 7297-7319.
16. Massoli, P.; Stark, H.; Canagaratna, M. R.; Krechmer, J. E.; Xu, L.; Ng, N. L.; Mauldin, R. L., III; Yan, C.; Kimmel, J.; Misztal, P. K.; Jimenez, J. L.; Jayne, J. T.; Worsnop, D. R., Ambient Measurements of Highly Oxidized Gas-Phase Molecules during the Southern Oxidant and Aerosol Study (SOAS) 2013. *ACS Earth and Space Chemistry* **2018,** *2* (7), 653-672.
17. Liu, Y.; Liu, C.; Nie, W.; Li, Y.; Ge, D.; Chen, L.; Zhu, C.; Wang, L.; Zhang, Y.; Liu, T.; Qi, X.; Wang, J.; Huang, D.; Wang, Z.; Yan, C.; Chi, X.; Ding, A., Exploring condensable organic vapors and their co-occurrence with PM2.5 and O3 in winter in Eastern China. *Environmental Science: Atmospheres* **2023,** *3* (2), 282-297.
18. Shen, H.; Vereecken, L.; Kang, S.; Pullinen, I.; Fuchs, H.; Zhao, D.; Mentel, T. F., Unexpected significance of a minor reaction pathway in daytime formation of biogenic highly oxygenated organic compounds. *Science Advances* **2022,** *8* (42), eabp8702.
19. Liu, Y.; Nie, W.; Li, Y.; Ge, D.; Liu, C.; Xu, Z.; Chen, L.; Wang, T.; Wang, L.; Sun, P.; Qi, X.; Wang, J.; Xu, Z.; Yuan, J.; Yan, C.; Zhang, Y.; Huang, D.; Wang, Z.; Donahue, N. M.; Worsnop, D.; Chi, X.; Ehn, M.; Ding, A., Formation of condensable organic vapors from anthropogenic and biogenic volatile organic compounds (VOCs) is strongly perturbed by NO_x in eastern China. *Atmospheric Chemistry and Physics* **2021,** *21* (19), 14789-14814.